5th International Conference on Experimental Fluid Mechanics ICEFM 2018 Munich
Munich, Germany, July 2-4, 2018

Optimized Experimental Environment for Wing Profile Investigations in the Low Speed Wind Tunnel

Oliver Meyer[1*], Tasha Terreblanche[2], Michael Klein[2]

[1] Universität der Bundeswehr München, Dept. of Mechanical Engineering, Neubiberg, Germany

[2] TEG Tubercle Engineering Group GmbH, Munich, Germany

[*] oliver.meyer@unibw.de

Abstract

The experimental environment in the low speed wind tunnel of the Universität der Bundeswehr München (UniBwM) was optimized to perform basic 2D blade profile tests in an open test section. The major changes and developments are the optimization of the streamwise static pressure gradient in the test section, the adaptation of existing profile models with the use of end plates as well as the design and use of a wake rake. Additionally, surface oil flow and infrared visualization techniques were utilized to visualize the surface flow on the models and to validate the general flow characteristics on the profiles. The whole process to determine a profile polar now takes less than 1h including model exchange. The test results for two reference laminar profiles were validated against results in a large wind tunnel and XFOIL. The results show a very good coincidence in lift and lift gradient over a large angle of attack range after appropriate wind tunnel interference corrections have been applied to the measured data. The UniBwM wind tunnel will be used in the future for the pre-development of stall-optimized wind turbine rotor blade profiles with different leading edge modifications and devices.

1 Introduction

The low speed wind tunnel of the Dept. of Mechanical Engineering of the UniBwM had to be optimized to investigate 2D wing profiles. The aim is to obtain lift and drag polars from satisfactory measurements over an angle of attack range from $\alpha = -20^\circ$ to $\alpha = 25^\circ$ at the maximum achievable Reynolds number. The profile models used have a chord length of $c = 0.35\,\mathrm{m}$ and a span of $b_m = 0.8\,\mathrm{m}$. The following tasks have been identified to optimize the existing testing environment for the intended profile tests:

- Identification and optimization of wind tunnel flow quality.
- Appropriate Installment of the given models in the test section.
- Realize a 2D profile flow in the open test section.
- Measure drag and lift forces through the required angle of attack range.
- Implement wind tunnel correctional methods for lift and drag.
- Validate the obtained results against reference data.

2 Wind Tunnel and Flow Quality

The wind tunnel at the department of mechanical engineering was build in 1975 and has undergone several modifications since. Some modifications implemented include the switch from a circular nozzle outlet to a rectangular nozzle, the implementation of a ground simulation by a moving belt, the insertion of acoustic splitter plates in the airline and a modern control system by ABB. The layout and the technical parameters of the tunnel are shown in figure 1. However, it is important to know the turbulence level Tu, the variation of the axial static pressure $c_p = f(x)$ in the centreline of the test section and the test section blockage ratio

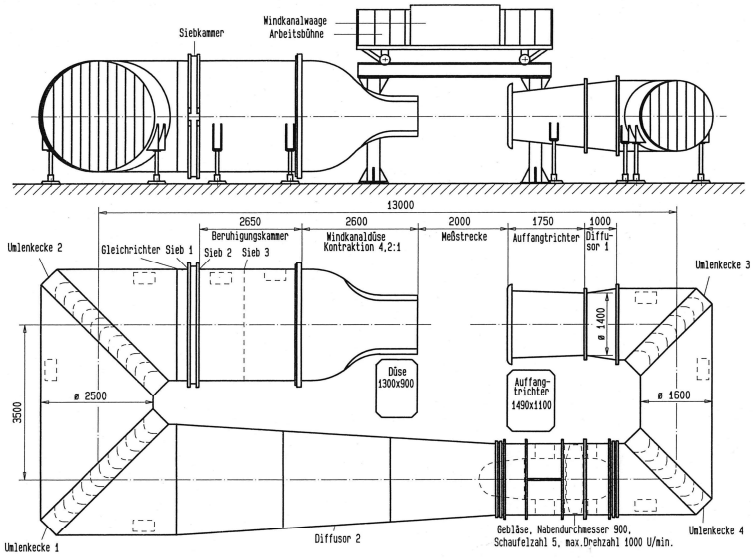

Wind Tunnel Data

Test Section (h x w x l)	0.9m x 1.3m x 2m
Velocity	0 - 40 m/s
Test Section Re-nr.:	$2.8 \cdot 10^6$
Power	75kW
Turbulence	0.35%
Ground Simulation (Belt with BL Removal System)	0-40 m/s
Axial Static Pressure Gradient	$\frac{dc_p}{dx} < \frac{0.002}{0.1m}$

Balance Data

Component	Range [N]	Resolution [N]	Max dev. from value
Drag I	0 - 100	0,1N	0.24%
Drag II	0 - 100	0,1N	0.32%
Lift I	0 - 200	0,1N	0.02%
Lift II	0 - 200	0,1N	0.02%
Lift III	0 - 200	0,1N	0.02%
Lateral	0 - 100	0,1N	0.32%

Figure 1: The Wind Tunnel of the Department of Mechanical Engineering

B (model to nozzle cross sectional area) for the intended profile tests in order to determine whether the intended tests can be performed or not.

Typically, open test sections show a certain axial pressure gradient, which directly influences the measurement results, SAE (1999). Fig. 2 shows the axial static pressure distribution in the centreline of the test section before (upper lines) and after optimization (lower lines) for two velocities each, Eder (2015). The flow experienced a dominant negative axial pressure gradient from the nozzle (left) almost up to the reference position in the test section. The typical positive static pressure gradient to the collector entry (right) was less dominant. However, a small inclination of the Seiferth-Wings at the nozzle exit of appr. 5° in outboard direction reduced the negative axial pressure gradient in the front section of the test section very efficiently and the use of small collector wings reduced the gradient in the rear section. The utilization of collector wings in open jet wind tunnels is shown for example by Duell et al. (2010). The collector wings could not be used for the planned profile testing, because they limit the required test section length. Therefore, resulting gradient effects in this area must be included in the applied correctional methods.

The turbulence in the test section was determined by hot wire anemometry and measurements with a pressure sphere. Hot wire measurements yielded a turbulence level of appr. $Tu = 0.35\,\%$ over the speed

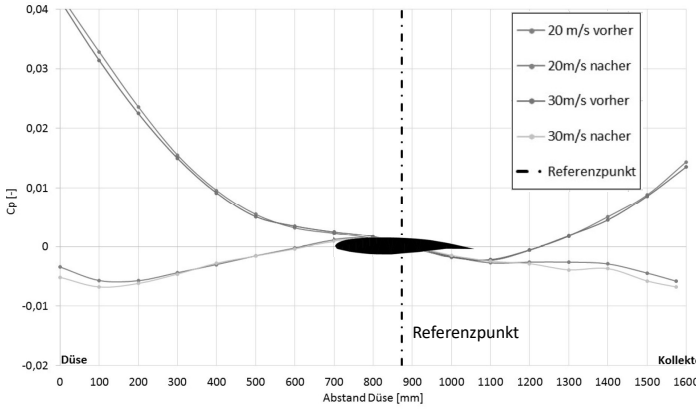

Figure 2: Static pressure gradient in test section with model before and after optimization, Eder (2015)

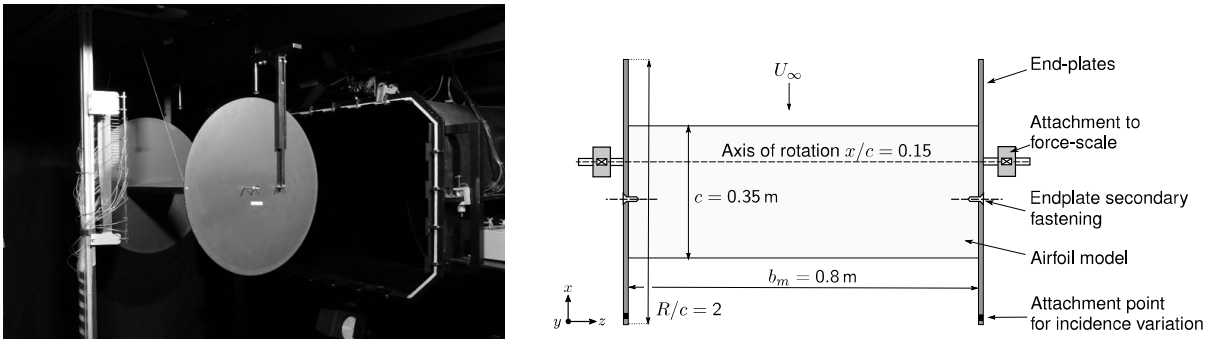

(a) Overview, profile with end plates in test section

(b) Top view, Terreblanche (2017)

Figure 3: Test setup

range of the wind tunnel in the reference position of the test section, Eulitz (2014). Measurements with a pressure sphere, like described by Ratakrishnan (2017), yielded comparable results.

The testing Reynolds number is appr. $Re = 0.8 \cdot 10^6$ for the given profile length of $c = 0.35\,\mathrm{m}$ and a maximum testing speed of $u_\infty = 40\,\mathrm{m/s}$ in the given environment. The blockage ratio is appr. $B = 7\,\%$ for the given profiles, regarding the new effective test section width of $b_m = 0.8\,\mathrm{m}$ with the addition of end plates. The test section is a quasi open test section, open to the ceiling and floor.

3 Test Section and Airfoil Model Setup

In order to realize a 2D flow over the model within the open test section, circular end plates were designed and fixed to the airfoils which move with the profile through the angle of attack range. Fig. 3(a) shows the profile with end plates in the test section and a wake rake located behind the profile. The model was mounted to an external overhead balance system, which allowed an angle of attack variation via the vertical movement of the rear lift balance to which the model was fixed with steel wires. The top view of the setup is schematically shown fig. 3(b).

The end plates were designed with a diameter twice the model chord length of the profiles, which proved to deliver acceptable results: Fig. 4 shows the flow pattern on a profile visualized by surface oil flow technique, tufts and the use of an infrared thermography camera (IRT). The 2D nature of the main profile flow is obvious. A laminar separation bubble was present for the used laminar profile on the pressure and suction side at low angles of attack. The separation bubble on the suction side is visible in fig. 4(a) and 4(c) at a position on the profile of appr. $x/c = 0.5$. The separation bubble formed a distinct and straight separation and turbulent reattachment line which is clearly visible in the surface oil flow patterns and even clearer in the IRT pictures. The region directly at the end plates was influenced by the development of a horseshoe vortex which was formed at the profile root, observed in the oil flow pattern. Appr. 2.5 % of the span was affected by this interference at a relative chord length of $x/c = 0.5$. Thus appr. 91 % of the entire wing area was not affected by end plate interference effects for the given profile in the position of zero lift.

4 Lift and Drag Measurement

The lift measurements were performed with the external overhead balance of an AVA-Göttingen type, see also Wuest (1969). The technical data is listed in fig. 1. Drag measurements were not to be performed with the balance, since the required correction of the model suspension drag was too dominant compared to the actual profile drag. Therefore, a wake rake was build and used to derive the profile drag through the analysis of the momentum loss in the wake of the profile. The wake rake was positioned relatively close to the model trailing edge with a distance of $x/c = 0.6$ which required the measurement of both the static- and total pressure in the profile wake, Wuest (1969). The profile drag derivation was realized by the formula of

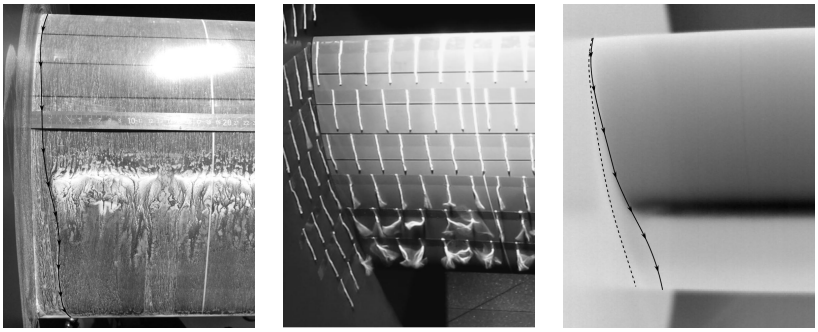

(a) Surface oil flow (b) Tufts (c) Infrared thermography

Figure 4: Vizualisation of end plate effects and 2D nature of profile flow, Terreblanche (2017)

Jones (1936):

$$c_d = 2 \int_{-\infty}^{\infty} \sqrt{\frac{p_t - p_s}{q_\infty}} \left(1 - \sqrt{\frac{p_t - p_{s,\infty}}{q_\infty}} \right) \mathrm{d} \left(\frac{y}{c} \right) \tag{1}$$

The used wake rake measured the total and static pressure behind the profile via pitot and static tubes. The pitot tubes measured the total pressure up to a flow angle of 7° within an accuracy of appr. 1 %, Nitsche and Brunn (2006) and Terreblanche (2017). A correction may be applied for larger flow angles. The effective flow angles at the vertical position of the pitot tubes were estimated by potential flow calculation. The circulation of the profile was derived at different angles of attack and the effective flow angles in the various positions of the pitot tubes were calculated with the Biot-Savart-Law. These estimations showed a local flow angle deviation between 4° to 14° over the length of the rake for an angle of attack of the profile of $\alpha = 11°$. A maximum flow angle at the pitot tubes of 14° was estimated for the planned experiments with a corresponding error in total pressure of appr. 5 %. The corresponding error in static pressure was estimated in the region of appr. 8 %. However, the wake measurement is still an error source for drag measurements at higher angles of attack of appr. $\alpha > 7°$. The measurement will be optimized with a new, flow angle calibrated wake rake, flow angle measurements at the rake and flow angle corrections for the measured pressures. The investigation of a rake which moves with the inclination of the wing is also planned.

5 Wind Tunnel Corrections

Various wind tunnel correctional procedures have been investigated to correct the measured polars due to the acting interference effects in this model setup. It was shown by Terreblanche (2017) that the correction for lift is most successfully performed with the method of Rae et al. (1999). The best drag correction in magnitude at small angles of attack was achieved with the method described and summarized in Mercker (2013). The method was initially derived for vehicle testing in open test section wind tunnels, i.e for bluff bodies of revolution. This method corrects in sum for five single interference effects, namely nozzle blockage, solid blockage/jet expansion, collector blockage, pressure gradient and wake distorsion. But the overall shape of the drag polar appears too distorted to perform the intended profile optimizations. Therefore, also the method of Rae et al. (1999) is applied to the drag measurements, because the shape of the polars remains comparable to the reference data, but with a relatively constant offset, see chapter 6.

6 Validation of Measurements

The validation measurements were performed for two reference laminar profiles characterized in table 1. The results for the TEG4418 profile in the UniBwM wind tunnel and results from XFOIL calculations were validated against reference wind tunnel data from the Laminar Wind Tunnel of the IAG in Stuttgart, fig. 5. The reference wind tunnel data for the TEG4418 profile were measured at $Re = 1.1 \cdot 10^6$ whereas the planned tests could only be performed at max. $Re = 0.8 \cdot 10^6$. Additionally, the turbulence level in the IAG wind tunnel was much smaller ($0.02\,\% \leq Tu \leq 0.05\,\%$). Hence, a certain difference in the results was expected.

Table 1: Basic design information of the used validation profiles

Airfoil	Maximum thickness t [%·c]	Point of maximum thickness $x_{t,max}$ [%·c]	Leading edge radius r_{LE} [%·c]	Cross-sectional area A_z [%·c]
TEG4418	18.00	40.9	1.42	11.38
TEG2618	18.37	35.1	1.96	11.51

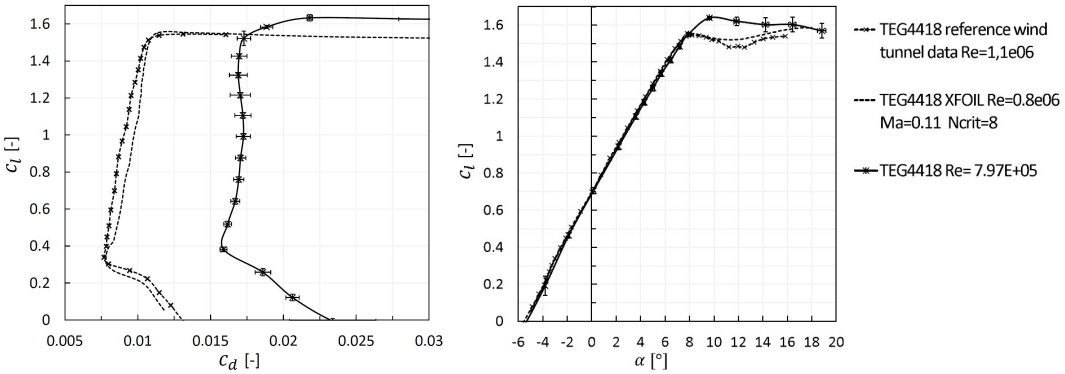

Figure 5: Comparison of the TEG4418 UniBwM profile polars with the wind tunnel reference data of the IAG Stuttgart and XFOIL, Terreblanche (2017)

XFOIL was validated against the reference data with the Reynolds number of $Re = 1.1 \cdot 10^6$ where the 'critical amplification factor' N_{crit} was adjusted to the wind tunnel. For the description of XFOIL see Drela and Youngren (2001). XFOIL shows only minor deviations from the reference data, both in drag and lift. The corrected wind tunnel data showed a relatively constant offset in drag over the angle of attack range plus an additional offset at higher angles of attack which can be attributed to the wake rake errors discussed in chapter 4. The Reynolds sensitivity of the laminar separation bubble influenced the results additionally, see Terreblanche (2017). The lift polars of the reference data and XFOIL match remarkably well. The UniBwM lift polar also coincides very well with the reference data in a large angle of attack range, with a deviation only visible in the region of maximum lift.

Both the test results for the TEG2618 from the UniBwM as well as the corresponding XFOIL calculations were validated against reference wind tunnel data from the Deutsche WindGuard in Bremerhaven, see fig. 6. This wind tunnel has a turbulence level of $Tu = 0.35\,\%$ which is similar to the UniBw wind tunnel. XFOIL shows the lowest drag over the shown angle of attack range and the UniBwM results show the highest drag. Because of this deviation, future profile testing at the UniBwM may focus on relative changes from a baseline design and not on absolute values in drag.

However, the corrected lift polars measured in the UniBwM wind tunnel and in particular the zero lift angle and the lift gradient coincide very well with the reference data. A deviation is visible in the regions of maximum lift. The deviations may be addressed to the larger test section interferences at high angles of attack and Reynolds-dependent effects.

7 Conclusion

The main flow quality parameters were determined in the low speed wind tunnel test section of the Universität der Bundeswehr München and the axial pressure gradient was successfully minimized. The test setup for 2D profile testing was optimized to ensure a 2D flow which was validated with different surface flow visualization techniques. Finally, the whole setup was tested with two profiles against reference wind tunnel data and XFOIL calculations which shows good agreement in the lift polars. The accuracy in drag measurement still suffers from the wake pressure measurement at higher angles of attack, the applied correctional method, the mismatch in the Reynolds number as well as different turbulence levels. However, effects in the lift behaviour of profile modifications can be analysed in the UniBwM wind tunnel and relative changes in the drag polars can also be measured to develop future profiles.

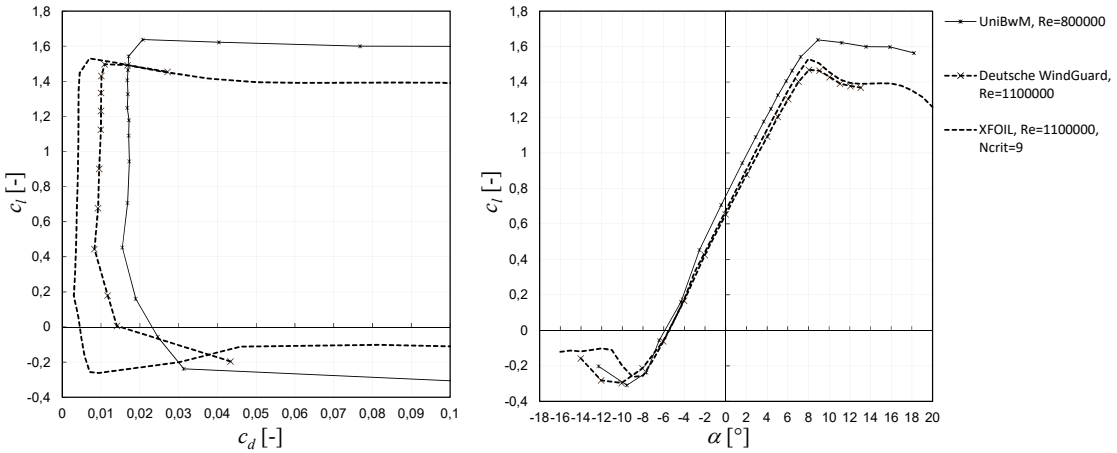

Figure 6: Comparison of the TEG2618 UniBwM profile polars with the wind tunnel reference data of WindGuard and XFOIL

Acknowledgements

This work was funded by the TEG Group.

References

Drela M and Youngren H (2001) *XFOIL 6.9: General Description*. MIT, Cambridge, USA

Duell EG, Kharazi A, Muller S, Ebeling W, and Mercker E (2010) The BMW AVZ Wind Tunnel Center. in *SAE, Vehicle Aerodynamics 2010*. 2010-SP-2269

Eder C (2015) *Optimierung des Druckgradienten im großen Windkanal durch Optimierung des Kollektors*. Master's thesis. Universität der Bundeswehr München

Eulitz R (2014) *Turbulenzgradmessung im großen Windkanal*. Master's thesis. Universität der Bundeswehr München

Jones M (1936) *Measurement of Profile Drag by the Pitot-Traverse Method*. London

Mercker E (2013) On Buoyancy and Wake Distorsion in Test Sections of Automotive Wind Tunnels. *Progress in Vehicle Aerodynamics and Thermal Management* pages 205–277

Nitsche W and Brunn A (2006) *Strömungsmesstechnik*. Springer, Berlin Heidelberg

Rae WH, Pope A, and Barlow JB (1999) *Low Speed Wind Tunnel Testing*. John Wiley and Sons, Inc.

Ratakrishnan E (2017) *Instrumentation, Measurements and Experiments in Fluids*. Taylor and Francis Group, LLC

SAE (1999) *Aerodynamic testing of road vehicles in open jet wind tunnels*. SP-1465. Society of Automotive Engineers

Terreblanche T (2017) *Optimization of Profile Polars for Wind Turbine Rotor Blades with the Use of Leading-Edge Vortex Generators*. Master's thesis. TU Braunschweig

Wuest W (1969) *Strömungsmeßtechnik*. Vieweg & Sohn GmbH, Braunschweig